Combined tidal and wind driven flows and residual currents

[1]Lars Erik Holmedal, Hong Wang

Abstract : The effect of a residual current on the combined tidal and wind driven flow and the resulting bedload sediment transport in the ocean has been investigated, using a simple one dimensional two-equation turbulence closure model. This model has been verified against field measurements of a tidal flow in the Celtic Sea. These data contained a tidal drift which has been predicted by the present model using different combinations of wind and tidal forcing with and without residual current. The results reveal that this tidal drift is mainly caused by the residual current. Predictions of the combined tidal and wind driven flow with given residual currents are presented, showing that the residual current has a substantial effect on both the depth averaged mass transport and the mean bedload transport directions; in some cases the effect of the residual current is to almost reverse the mean bedload transport direction. The residual current affects the rotation of the flow due to the Coriolis effect in the lower part of the water column (the near-surface flow is wind dominated), causing a larger or smaller clockwise rotation of the depth averaged mass transport, depending on the direction of the residual current. Finally, the bottom roughness is observed to have a small effect on the surface drift and the depth averaged mass transport.

Keywords : Tidal flows, Residual currents, Oscillating boundary layers, Wind driven flows, Ekman layer, Bedload transport

1 Introduction

In a previous work (Holmedal and Myrhaug, 2013) the combined tidal and wind driven flow at intermediate water depths was investigated using a simple tidal model. This model was validated against field measurements tabulated by King et al. (1985) of a tidal flow in the Celtic Sea over a flat bottom at 120 meters water depth. These field measurements were conducted by Richard Soulsby in 1983, tabulated in a technical report by King et al. (1985), and published by Soulsby (1990). The interactions between the strength and direction of the wind and the tidal forcing, as well as the effect of the bottom roughness and the Earth's rotation, were investigated. It was shown that the presence of the wind leads to a net sediment transport near the bottom which does not exist for a pure tidal flow where the particle trajectories are closed ellipses. King et al. (1985) detected residual currents (i.e. non-zero mean velocities averaged over the tidal cycle) at each elevation in the water column. These residual currents reveal the presence of a small tidal drift in the ocean. By accounting for the residual currents in the free stream velocity and taking into account the wind stress, Holmedal and Myrhaug (2013) found a fair agreement between the predictions and the measurements. A further investigation reveals that the tidal drift is mainly caused by the residual current, although the simulations also show that the wind direction is important for the direction of the drift through the water column.

The impact on residual currents on tidal flows has been investigated in numerous works. Among these are: Harris and Collins (1991); sediment transport paths in the Bristol Channel; Gao and Collins (1997); sediment transport caused by asymmetrical tidal forcing in conjunction with wave action; Fry and Aubrey (1990) found that tidal asymmetry in shal-

[1]Corresponding author. Email: lars.erik.holmedal@ntnu.no Phone (+47) 64 84 47 30 Fax: (+47) 73 59 56 97

low embayments can cause net sediment transport; Ransinghe and Pattiaratchi (2006) found that tidal asymmetry in inlets were more important for the net sediment transport than the occurances of flood or ebb dominant diurnal tides; Maren and Gerritsen (2012) conducted simulations of tidal flows in the Singapore Straits and found that finer and coarser sediments were transported in different directions, since the transport of finer sediments were dominated by residual currents while the transport of coarser sediments were governed by the tidal asymmetry. Moreover, Pritchard and Vieira (1984) measured non-tidal current velocities in the Cheasapeake Bay and found that the residual currents were related to the wind setting up a surface slope causing a pressure gradient acting against the wind direction. Fletcher et al. (2006) applied a three-dimensional ocean circulation model to investigate suspended load and bedload transport in a tidal inlet in Florida; their predicted sediment patterns were in qualitatively agreement with the observations. Similar kind of results were reported by Yu et al. (2011) for the Bay of Fundy, Canada.

The purpose of the present work is to investigate the effect of residual currents on the combined tidal and wind driven flow and the resulting sediment transport at intermediate water depths, relevant to near-coastal waters. It will be shown that the residual currents have a large impact both on the direction of the mean (averaged over a tidal period) depth averaged velocity and on the bedload sediment transport, while the direction of the mean surface velocity is less affected. Visualizations of the bedload transport are provided using the near-bed tidal ellipse. The effect of residual currents on the combined tidal and wind driven flows has, to the author's knowledge, not been investigated in detail in an idealized setting. Overall, the present work yields new insight into combined tidal and wind driven flows, and represents an extension to the work by Holmedal and Myrhaug (2013).

2 Model formulation

2.1 Governing equations

The tidal turbulent flow is modelled as a horizontally uniform boundary layer where the tidal forcing is driven by the mean ocean surface slope oscillating with the tidal frequency. The Reynolds-averaged equations for conservation of the mean momentum and mass become

$$\frac{\partial u}{\partial t} = -\frac{1}{\rho}\frac{\partial p}{\partial x} + \frac{\partial}{\partial z}(\nu_T \frac{\partial u}{\partial z}) + fv \quad (1)$$

$$\frac{\partial v}{\partial t} = -\frac{1}{\rho}\frac{\partial p}{\partial y} + \frac{\partial}{\partial z}(\nu_T \frac{\partial v}{\partial z}) - fu \quad (2)$$

where u and v are the horizontal velocity components, p is the pressure, ρ is the density of the water, ν_T is the kinematic eddy viscosity, f is the Coriolis parameter, and g is the gravity acceleration. The turbulence closure is given by a $k-\epsilon$ model using the logarithmic wall law near the rough bottom (see e.g. Rodi, 1993)

$$\frac{\partial k}{\partial t} = \frac{\partial}{\partial z}(\frac{\nu_T}{\sigma_k}\frac{\partial k}{\partial z}) + \nu_T\Big((\frac{\partial u}{\partial z})^2 + (\frac{\partial v}{\partial z})^2\Big) - \epsilon \quad (3)$$

$$\frac{\partial \epsilon}{\partial t} = \frac{\partial}{\partial z}(\frac{\nu_T}{\sigma_\epsilon}\frac{\partial \epsilon}{\partial z}) + c_{\epsilon 1}\frac{\epsilon}{k}\nu_T\Big((\frac{\partial u}{\partial z})^2 + (\frac{\partial v}{\partial z})^2\Big) - c_{\epsilon 2}\frac{\epsilon^2}{k} \quad (4)$$

where k is the turbulent kinetic energy and ϵ is the turbulent dissipation rate. The kinematic eddy viscosity is given by

$$\nu_T = c_1 \frac{k^2}{\epsilon}. \tag{5}$$

where the standard values of the model constants have been adopted, i.e. $(c_1, c_{\epsilon 1}, c_{\epsilon 2}, \sigma_k, \sigma_\epsilon)$ = (0.09, 1.44, 1.92, 1.00, 1.30).

The bedload sediment transport is given by a formula by Nielsen (1992)

$$\Phi = 12\theta^{\frac{1}{2}}(\theta - \theta_c)\frac{\theta}{|\,\theta\,|} \tag{6}$$

where

$$\Phi = \frac{q_b}{(g(s-1)d_{50}^3)^{\frac{1}{2}}} \tag{7}$$

$$\theta = \frac{\tau_{\rm b}}{\rho g(s-1)d_{50}} \tag{8}$$

Here q_b is the instantaneous dimensional bedload transport, $\tau_{\rm b}$ is the dimensional instantaneous sea bed shear stress, $s = 2.65$ is the density ratio between the bottom sediments and the water, and d_{50} is the median grain size diameter. The critical Shields parameter $\theta_c = 0.05$ must be exceeded for bedload transport to take place.

2.2 Boundary conditions and tidal forcing

The sea bed is assumed to be hydraulically rough, and a logarithmic wall law is applied here in conjunction with zero velocity at the bottom A wind stress τ_s is specified at the surface and is related to the wind speed 10 meters above sea surface (U_{10}) by the empirical relation $\tau_s = \rho_a\, c_{\rm d} U_{10}^2$, where $\rho_a = 1$ kg m^{-3} is the density of air and $c_{\rm d}$ is a friction factor. The forcing is assumed to be in the East-West direction (i.e. along the x-axis), while the wind direction is varied. Here the tidal forcing is driven by the mean ocean surface slope which is oscillating with the tidal frequency $\sigma = 2\,\pi/T_p$ where T_p is the tidal period. The assumption of hydrostatic pressure (following from the boundary layer approximation) yields

$$-\frac{1}{\rho}\frac{\partial p}{\partial x} = -g\frac{\partial \xi}{\partial x}\cos(\sigma t) \tag{9}$$

$$-\frac{1}{\rho}\frac{\partial p}{\partial y} = 0 \tag{10}$$

Here $\partial\xi/\partial x$ is the amplitude of the mean ocean surface slope.

2.3 Inclusion of residual currents

First the tidal boundary layer without wind is calculated freom Eqs.(1)-(5) using Eqs.(9) and (10). This yields the free stream velocities $U_0(t)$ and $V_0(t)$, taken from the vertical zone outside purely tidal boundary layer. These free stream velocities are applied to incoprorate residual currents. Due to the boundary layer approximation, the following relations applies:

$$-\frac{1}{\rho}\frac{\partial p}{\partial x} = \frac{\partial U_0}{\partial t} - fV_0 \qquad (11)$$

$$-\frac{1}{\rho}\frac{\partial p}{\partial y} = \frac{\partial V_0}{\partial t} + fU_0 \qquad (12)$$

When residual currents are considered, the tidal forcing in Eqs.(9) and (10) is replaced with the tidal forcing in Eqs.(11) and (12), using U_0 and V_0 obtained Furthermore, U_0 and V_0 in Eqs. (11) and (12) are substituted with i.e., $U_0 \pm U_s$ and $V_0 \pm U_s$ (depending on the direction of the residual current) where U_s is the magnitude of the residual current. The hydrostatic horizontal pressure gradients are then evaluated from Eqs. (11) and (12), using $U_0 \pm U_s$ and $V_0 \pm U_s$ instead of U_0 and V_0.

2.4 Numerical method

A finite difference method was used to solve the parabolic Eqs.(1-5) using second order central differences in space. Geometric stretching of the mesh was applied to obtain a fine resolution near the bed and close to the free surface; here 800 gridpoints were applied in the vertical direction. The spatial discretization of the equations for the horizontal velocity components, turbulent kinetic energy and dissipation rate give a set of stiff differential equations that were integrated simultaneously in time by the integrator VODE (Brown et al., 1989). Further details about the numerical methid are given in Holmedal and Myrhaug (2013).

3 Results and discussion

Residual currents may exist locally in the ocean, due to e.g. differences in temperature and salinity or by the presence of large-scale ocean currents. These residual currents may have a different direction from both the wind and the tidal forcing. Generally there is a co-existence of wind, tidal forcing and residual currents in the ocean, and for intermediate and shallow water depths, the interactions between these three components are important for both the local mass transport and sediment transport. Here the effect of the residual current on the combined tidal and wind driven flow and sediment transport is investigated.

The choice of parameters is similar to that of Holmedal and Myrhaug (2013), except for the presence of the residual current: The tidal period is 12.5 hours, the Coriolis parameter is $f = 1.112 \cdot 10^{-4} s^{-1}$, the amplitude of the mean ocean surface slope is given by $\partial \xi / \partial x = 3 \cdot 10^{-6}$ and the water depth is 120 m. The effect of the surface waves is represented as a surface roughness z_s ; in the present work this roughness is chosen as $z_s = 0.3$ cm. A sandy flat bottom, consisting of medium sand with $d_{50} = 0.21$mm, is considered; the bottom roughness is related to d_{50} by the empirical formula $z_0 = d_{50}/12$. The residual current towards the East or West has been taken into account by substituting U_0 with $U_0 \pm 0.02$ m/s in Eqs. (16) and (17) for residual current towards the East (+) or West (−). Similarly, the residual current towards the North or South has been taken into account by substituting V_0 with $V_0 \pm 0.02$ m/s for residual current towards the North (+) or South (−). In the present setting the effect of the wind is taken into account by specifying a wind stress at the surface as $\tau_s = 0.2$ Pa. For the stable and neutral atmospheric conditions more common in the Atlantic (using e.g. a friction factor $c_\mathrm{d} = 0.0015$), this wind stress correspond to U_{10} being 12 m/s, where U_{10} is the wind velocity 10 m above the ocean surface.

3.1 Effect of residual current on the depth averaged velocity

Figures 1-4 show the direction of the depth-averaged velocity, the surface drift and the mean bedload transport for 16 different combinations of specified wind and residual currents. Both the wind direction and the direction of the residual current are depicted in the each subfigure. The tidal forcing is in the East-West direction for all these cases. It is observed that for all the situations considered in Figs. 1-4, the surface drift is directed slightly to the right of the wind direction. This is consistent with the Ekman layer theory and also with the results obtained by Holmedal and Myrhaug (2013) for combined tidal and wind driven flows with no residual current. This shows that the surface drift is wind dominated; the residual current has little impact here. In the rest of this section the depth averaged velocity direction will be discussed; the mean bedload direction is discussed in the next Section.

Figure 1 shows four different situations where the residual current is co-directional with the tidal forcing and the wind is normal to the tidal forcing. It is well known that for Ekman flows the depth averaged velocity is 90 degrees to the right of the wind direction, also for turbulent flows. This result also holds for combined wind and tidally driven flows (Holmedal and Myrhaug, 2013), if the water depth is not to shallow. Figure 1 shows that the presence of the residual current changes this picture substantially. Overall, Figs. 1a-d show that the direction of the depth averaged velocity is nearly in the same direction as the residual current for the four situations in Fig. 1.

Figure 2 shows the situation where both the residual current and the wind are normal to the tidal forcing. The depth averaged velocity is closest aligned with the residual current direction, but the angle between the residual current and the depth averaged velocity is substantially larger than in Fig. 1. It should be noted that the depth averaged velocity is not directed 90 degrees to the right of the wind, as it would have been without the residual current.

The situations where both the residual current and the wind are colinear with the tidal forcing is shown in Fig. 3. Here the depth averaged velocity direction is strongly affected by the residual current. In Figs. 3a and d the depth averaged velocity is rotated less than 90 degrees to the right of the wind, while this rotation is more than 90 degrees in Figs. 3b and c. The reason is that the residual current affects the rotation of the flow due to the Coriolis effect in the lower part of the water column (the near-surface flow is wind dominated). This can be illustrated by a simple vector sum. Consider a given vertical elevation and given velocity components u and v for a wind driven flow. If for example $u > 0$ and $v < 0$, and a small positive residual current U_s is added to u, the resulting velocity vector $(u + U_s, v)$ will be less clockwise rotated than the velocity vector without the residual current (u, v), i.e. the residual current counteracts the rotation. However, if a small negative residual current $-U_s$ is added to u, the resulting velocity vector $(u - U_s, v)$ will be more clockwise rotated towards the right, i.e. the residual current increases the clockwise rotation. This explains the decrease of the clockwise rotation in Figs. 3a and d, and the increase of the clockwise rotation in Figs. 3 b and c, relative to the case of no residual current.

Figure 4 depicts the situations where the residual current is normal to and the wind is co-directional to the tidal forcing. As in Fig. 1, the depth averaged velocity is almost in the same direction as the residual current, i.e. here the residual current has a strong impact on the depth averaged velocity.

3.2 Effect of residual current on the bedload transport

If the resulting bottom shear stress magnitude is strong enough to move the sea bed material, or to bring it into suspension, sediment transport takes place either as suspended load or bedload. Holmedal and Myrhaug (2013) found that for tidal flows alone the particle trajectories consisting of closed ellipses show that there is a symmetry in the bedload. Hence the same amount of sand is moved along opposite trajectories; thus no net sediment transport takes place. For combined tidal and wind driven flows, where the near-bed particle trajectories are propagating ellipses, there is an asymmetry in the sediment transport along the trajectories, and hence a net sediment transport takes place if the magnitude of the bottom shear stress is large enough. In order to facilitate good predictions of the sediment transport beneath combined tidal and wind driven flows, a flat bottom consisting of medium sand with a median sand grain diameter of $d_{50} = 0.21$mm has been chosen; this coincides with the choice of Holmedal and Myrhaug (2013). For the present physical parameters the sediment transport takes place as bedload; a detailed discussion is given in Holmedal and Myrhaug (2013).

The effect of the residual current on the mean bedload transport direction is presented in Figures 1-4. For combined tidal and wind driven flows Holmedal and Myrhaug (2013, Fig. 13) found that the mean sediment transport is more aligned with the tidal forcing (East-West direction) than with the North-South direction, indicating that the tidal forcing is the dominating mechanism behind the bedload transport. They also found that the mean bedload transport direction was opposite (when projected to the East-West axis) to the wind direction. Also Figs. 1 and 3 show that when the residual current is directed along the axis of tidal forcing (regardless of the wind direction), the mean bedload transport direction (when projected to the East-West axis) follows that of the residual current. However, the mean bedload transport direction is closest aligned to the axis of tidal forcing (East-West), showing the importance of the tidal forcing.

When both the wind and the residual current are normal to the tidal forcing and act in the same direction (Figs. 2a and b), the mean bedload transport is aligned along the axis of tidal forcing, almost 90 degreees to the right of the wind and residual current. However, when the wind opposes the residual current (but is normal to the tidal forcing), a more complicated picture arises, and it appears that the wind has a substantial effect on the mean bedload transport direction. The reason for this is not clear to the authors, but the wind might change the phase of the tidal velocity, which again changes where in the tidal cycle the bottom shear stress is largest and where it exceeds the treshold value for bedload transport to take place. Figure 4 shows that when the redisual current is normal to and the wind is parallel to the tidal forcing, the mean bedload transport direction is opposite (when projected to the East-West axis) to the wind direction, i.e. similar to case without residual current presented in Holmedal and Myrhaug (2013).

Figure 5 shows the mean bedload transport direction for combined tidal and wind driven flow with and without a residual current; the directions of the wind and the residual current are also given. For residual current and wind in the same direction along the tidal forcing axis (Fig. 5a), the effect of the residual current is to almost reverse the direction of the mean sediment transport direction. However, the residual current has almost no impact on the mean sediment transport direction when the residual current is normal to and the wind is co-directional to the tidal forcing (Fig. 5b). The residual current has some impact on the mean sediment transport direction when it is co-directional to, and the wind is normal to -the tidal forcing (Fig. 5c). Finally, when both the residual current and the wind is normal to the tidal forcing, the mean sediment transport direction is substantially changed relative to the case of no residual current.

The near-bed trajectories for combined wind and tidally driven flows, with and without residual current, are presented in Fig. 6 and corresponds to the conditions in Fig. 5a-d with the tidal forcing is in the East-West direction. These near-bed particle trajectories are propagating ellipses; the particles move in the clockwise direction, starting in origo. The symbols (circles or crosses) on the tidal ellipse denote that bedload sediment transport takes place, i.e. that the Shields number exceeds the critical value for motion of sediments. No symbols indicates no bedload transport. For all the four cases it is clearly seen that the ellipses are propagating in the direction of the residual current (relative to the case of no residual current). As pointed out by Holmedal and Myrhaug (2013), the regions of no sediment transport are located in the Eastern or Western parts of the ellipses, regardless of the direction of the wind or the residual current. These are the regions where the particle trajectories are nearly normal to the tidal forcing and where the bottom shear stress is smallest, suggesting that the tidal forcing in the East-West direction is the dominant mechanism of the bedload transport. For both the wind and the residual current in direction of the tidal forcing (Fig. 6a), there is one Western and one Eastern region of no sediment tranport. When the residual current is normal to and the wind is co-directional to the tidal forcing (Fig. 6b), there is only one region of no bedload transport (to the East); when the residual current is co-directional with and the wind is normal to the tidal forcing (Fig. 6c), there is also only one region of no bedload transport (but here to the West). Finally, when both the wind and the residual current are normal to the tidal forcing, there is one Western and one Eastern region of no sediment tranport. It is also observed in Fig. 6b that there are two regions of no bedload transport when the residual current is absent, and one such region when it is present. However, Fig. 6d shows two regions of no bedload transport when the residual current is present, and one when it is absent.

Overall, the mean bedload transport direction results from a delicate balance between the tidal forcing, wind and residual current which yield different phases and directions of the bottom shear stress through the tidal cycle. The averaging over the tidal cycle is further complicated by the critical shear stress which must be exceeded for bedload transport to take place, giving regions of no sediment transport within the near-bed tidal ellipse. The results in Figs. 1-6 show that the mean bedload transport direction is overall more aligned with the axis of tidal forcing (East-West) than the North-South axis, demonstrating that the tidal forcing is a dominating mechanism of the bedload transport. However, the projection of the mean bedload transport direction on the East-West axis is always in the same direction as the residual current, when the residual current is directed along the East-West direction. When the residual current is normal to and the wind parallel to the tidal forcing, the impact of the residual current on the mean bedload transport direction appears to be weak. For those situations where both the residual current and the wind are normal to the tidal forcing, both the wind and the residual current affect the mean bedload transport.

4 Conclusions

Predictions of the combined tidal and wind driven flow with given residual currents are presented, showing that the residual current has a substantial effect on the depth averaged mass transport mean bedload transport directions:

- The surface drift is wind dominated with the direction slightly to the right of the wind.
- When the residual current is parallel to and the wind is normal to the tidal forcing, the direction of the depth averaged mass transport is nearly in the same direction as the residual current.
- When both the residual current and the wind are normal to the tidal forcing, the depth averaged mass transport is again aligned with the residual current direction (when projected to it).
- When both the residual current and the wind are colinear with the tidal forcing, there is a decrease of the clockwise rotation for residual current and the wind is in the same direction, and an increase of the clockwise rotation for residual current and the wind is in opposite direction, relative to the case of no residual current where the depth averaged velocity is 90 degrees to the right of the wind direction.
- When the residual current is normal to and the wind is co-directional to the tidal forcing, the depth averaged velocity is almost in the same direction as the residual current, i.e. here the residual current has a strong impact on the depth averaged velocity.

Overall, the mean bedload transport direction results from a delicate balance between the tidal forcing, wind and residual current which yield different phases and directions of the bottom shear stress through the tidal cycle. The averaging over the tidal cycle is further complicated by the critical shear stress which must be exceeded for bedload transport to take place, giving regions of no sediment transport within the near-bed tidal ellipse. The mean bedload transport direction is overall more aligned with the axis of tidal forcing (East-West) than the North-South axis, demonstrating that the tidal forcing is a dominating mechanism of the bedload transport. However, the projection of the mean bedload transport direction on the East-West axis is always in the same direction as the residual current, when the residual current is directed along the East-West direction (i.e. the along the axis of tidal forcing). When the residual current is normal to and the wind parallel to the tidal forcing, the impact of the residual current on the mean bedload transport direction appears to be weak. For those situations where both the residual current and the wind are normal to the tidal forcing, both the wind and the residual current affect the mean bedload transport.

Acknowledgement

This work was carried out as a part of the project 'Air-Sea Interactions and Transport Mechanisms in the Ocean' funded by the Norwegian Research Council. This support is gratefully acknowledged.

? ?

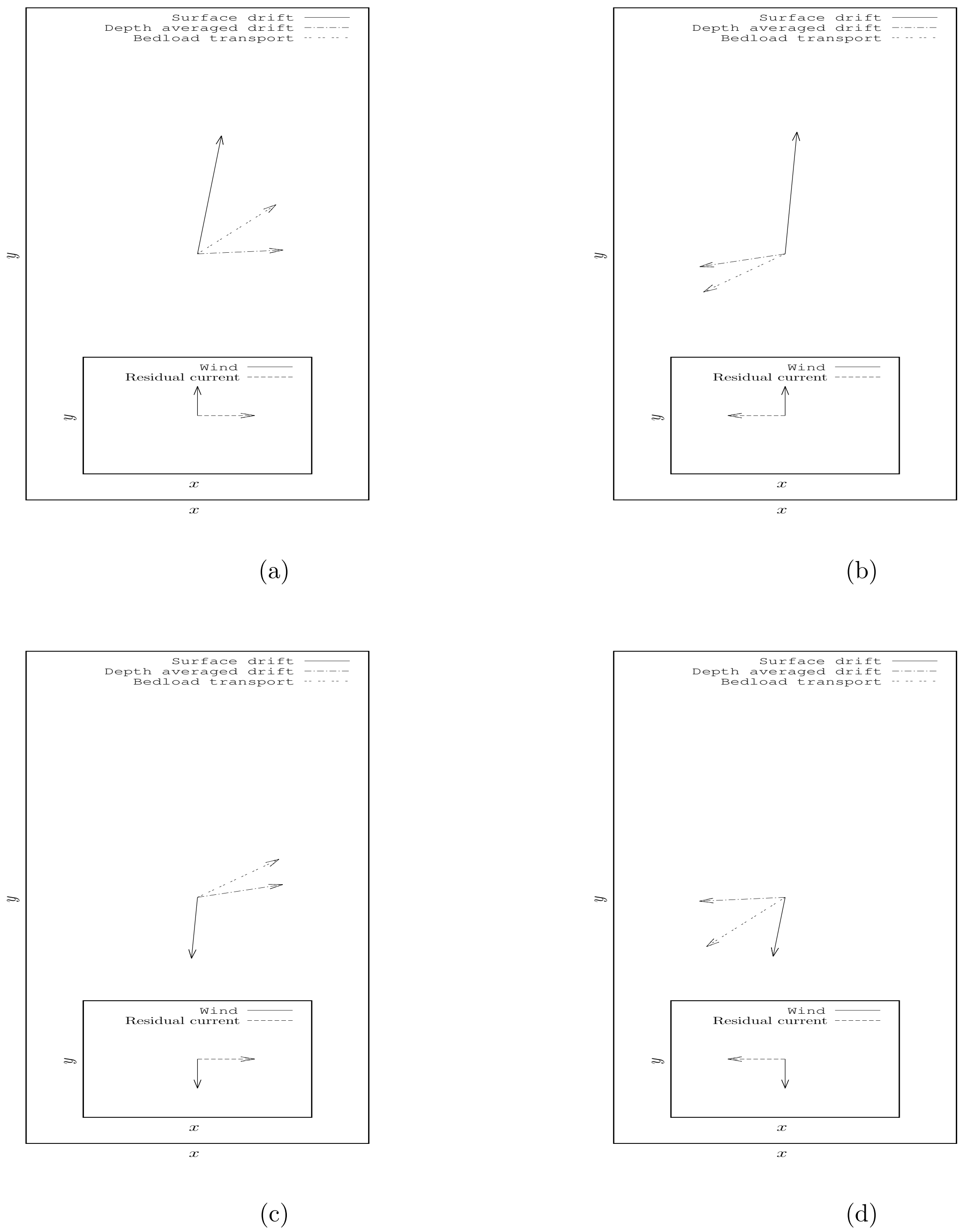

Figure 1: Directions of depth-averaged velocity, surface drift and bedload transport for the residual current parallel to tidal forcing and the wind direction normal to tidal forcing. The tidal forcing is in the East-West direction. Note that here only the direction of the quantities is given. The directions of the wind and the residual current are given in the small box.

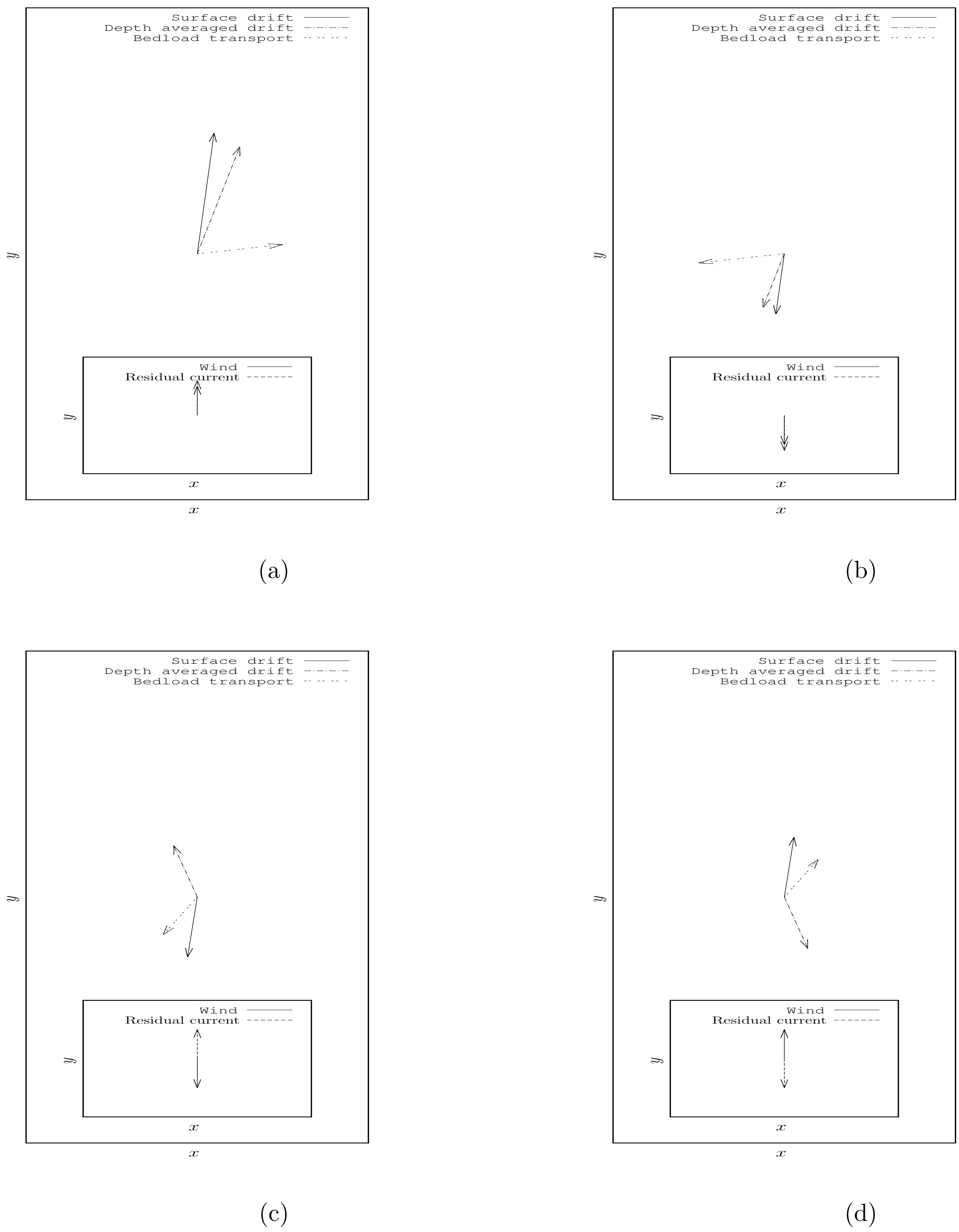

Figure 2: Directions of depth-averaged velocity, surface drift and bedload transport for both residual current and wind normal to the tidal forcing. The tidal forcing is in the East-West direction. Note that here only the direction of the quantities is given. The directions of the wind and the residual current are given in the small box.

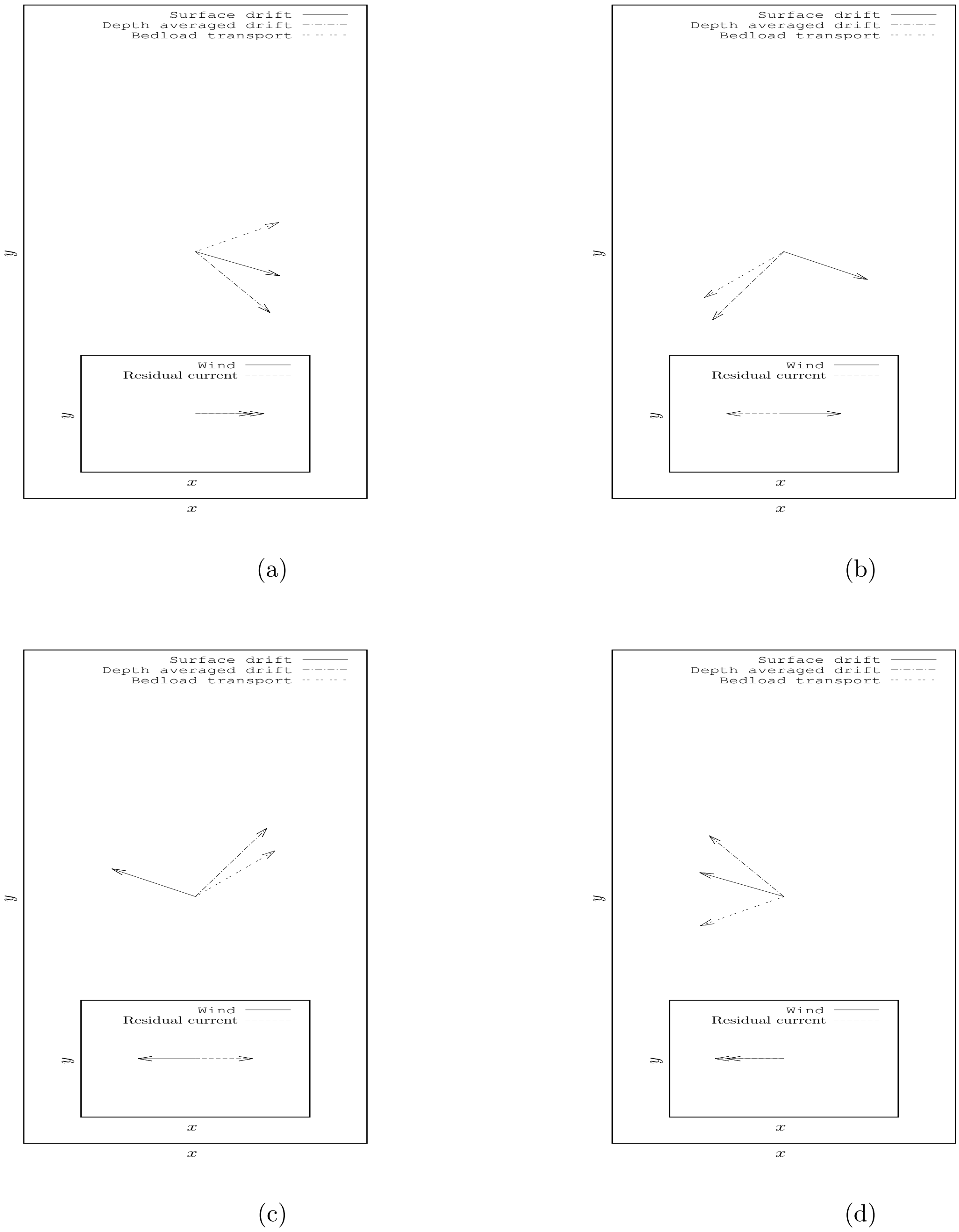

Figure 3: Directions of depth-averaged velocity, surface drift and bedload transport for both residual current and wind parallel to tidal forcing. The tidal forcing is in the East-West direction. Note that here only the direction of the quantities is given. The directions of the wind and the residual current are given in the small box.

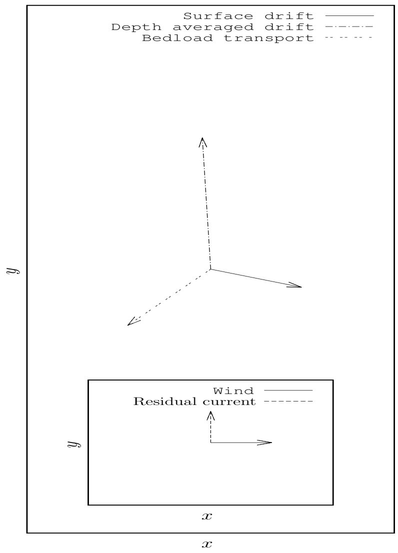

(a)

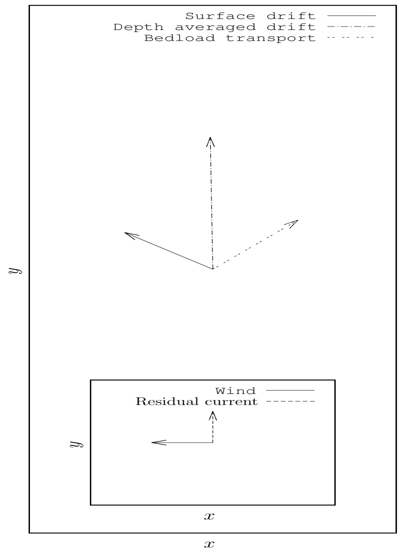

(b)

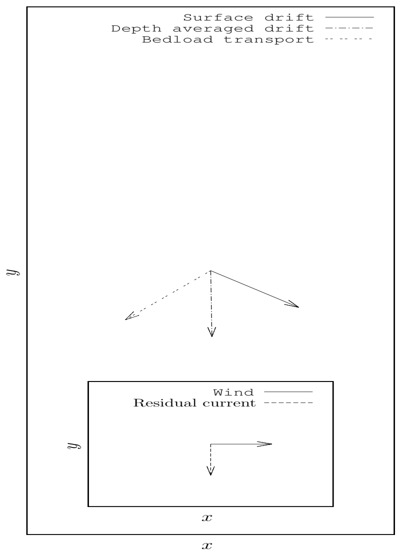

(c)

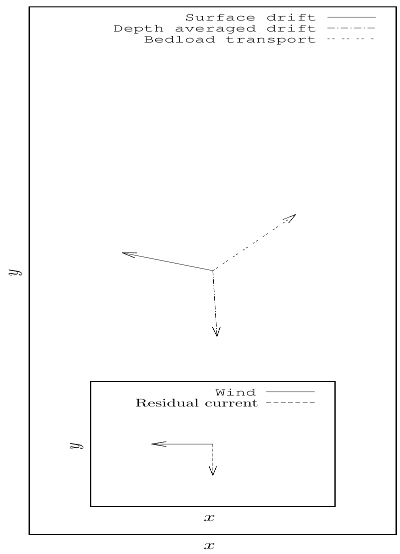

(d)

Figure 4: Directions of depth-averaged velocity, surface drift and bedload transport for the residual current normal to tidal forcing and wind parallel to tidal forcing. The tidal forcing is in the East-West direction. Note that here only the direction of the quantities is given.The directions of the wind and the residual current are given in the small box.

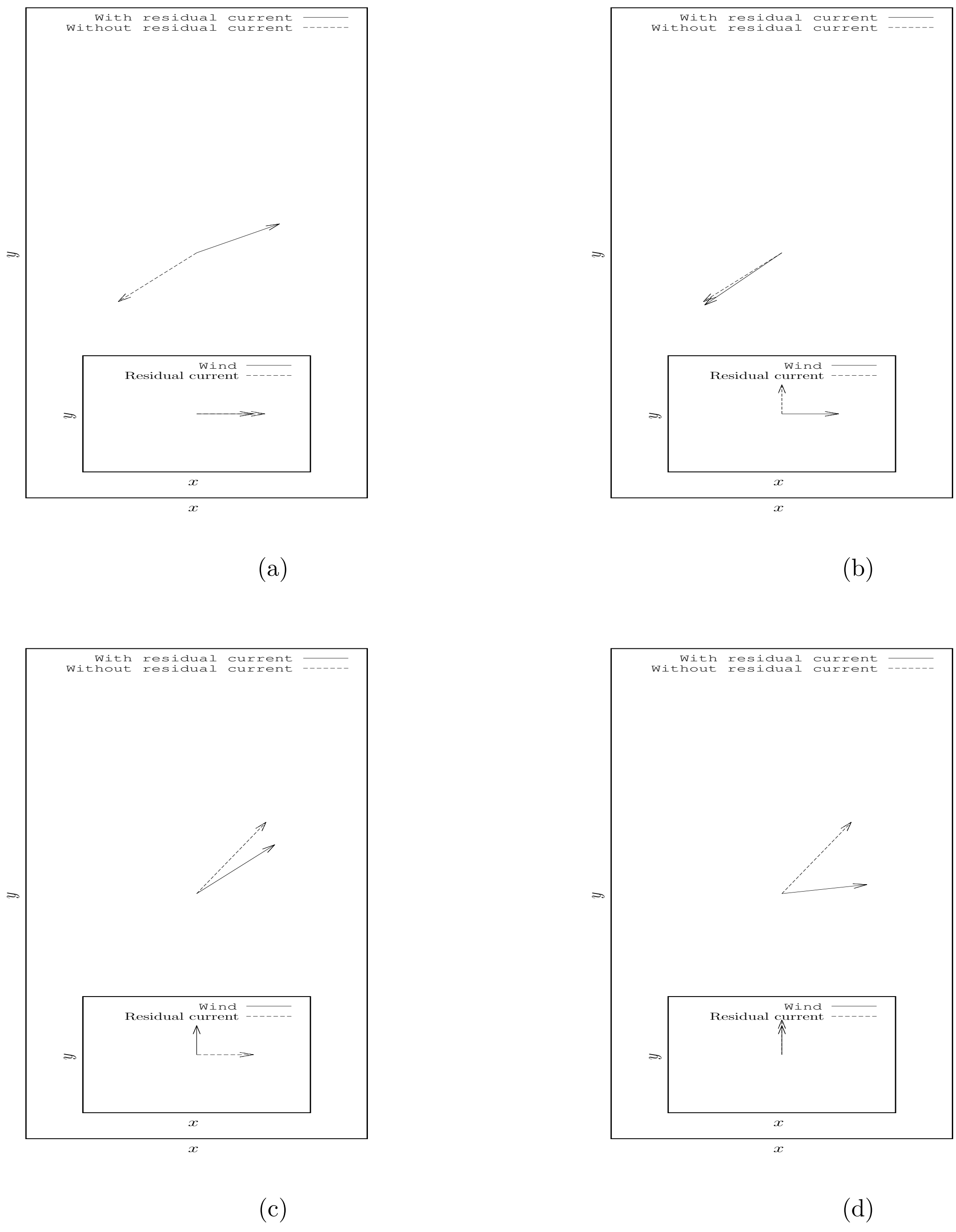

Figure 5: Directions of bedload transport for combined tidal and wind-driven flow with and without a residual current. The tidal forcing is in the East-West direction. Note that here only the direction of the quantities is given. The directions of the wind and the residual current are given in the small box.

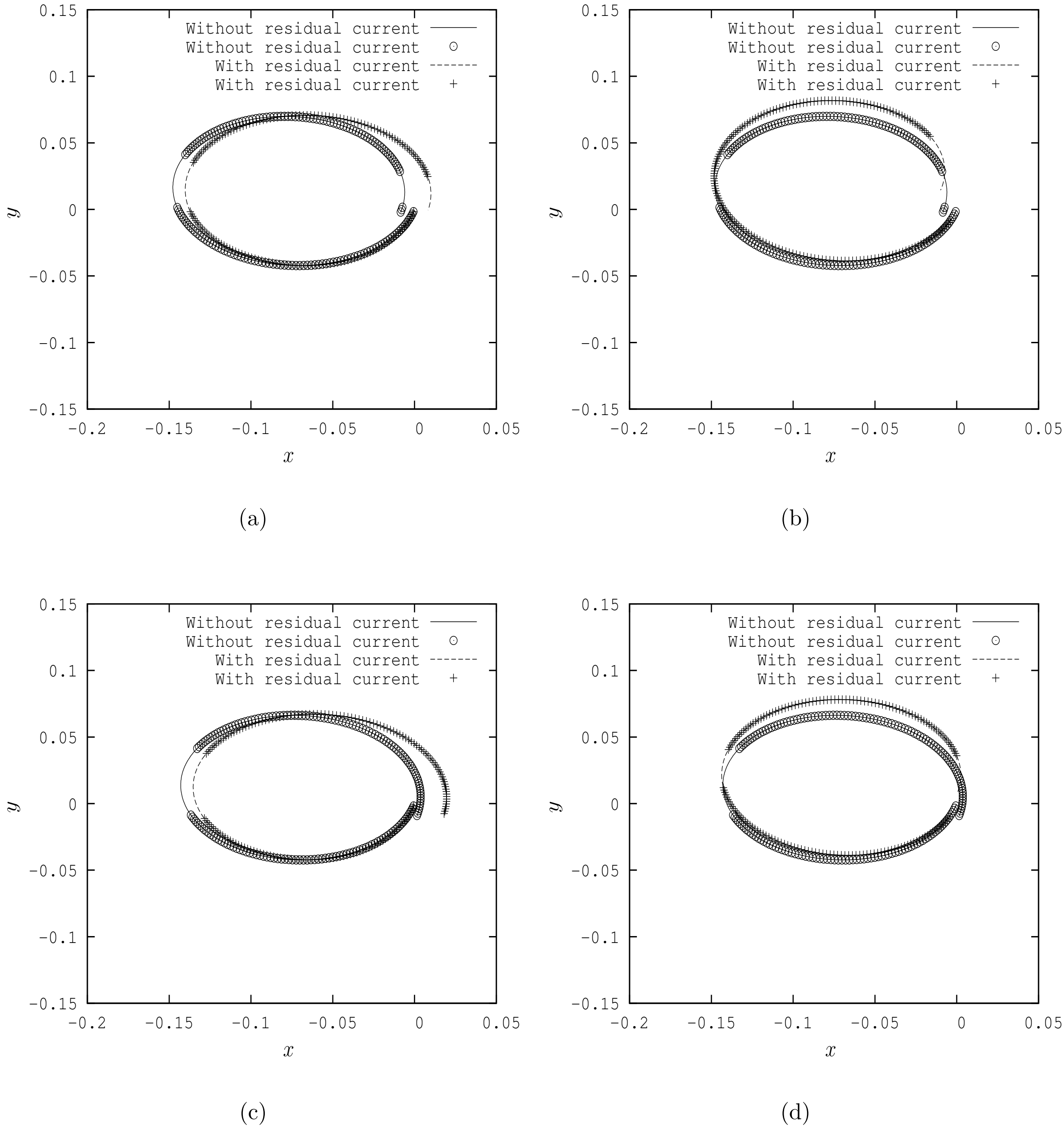

Figure 6: Near-bed tidal ellipses with bedload transport for combined tidal and wind-driven flow with residual current, corresponding to Figures 5 a,b,c and d. The full and dashed lines denotes the particle trajectories; the points show the part of the particle trajectories where sediment transport takes place. The tidal forcing is in the East-West direction.